The Influence of Land Use Change on Climate in the Sahel

CHRISTOPHER M. TAYLOR

Centre for Ecology and Hydrology, Wallingford, Oxfordshire, United Kingdom

ERIC F. LAMBIN AND NATHALIE STEPHENNE

University of Louvain, Louvain-la-Neuve, Belgium

RICHARD J. HARDING

Centre for Ecology and Hydrology, Wallingford, Oxfordshire, United Kingdom

RICHARD L. H. ESSERY

Met Office, Bracknell, Berkshire, United Kingdom

(Manuscript received 10 December 2001, in final form 14 June 2002)

ABSTRACT

A number of general circulation model (GCM) experiments have shown that changes in vegetation in the Sahel can cause substantial reductions in rainfall. In some studies, the climate sensitivity is large enough to trigger drought of the severity observed since the late 1960s. The extent and intensity of vegetation changes are crucial in determining the magnitude of the atmospheric response in the models. However, there is no accurate historical record of regional vegetation changes extending back to before the drought began. One important driver of vegetation change is land use practice. In this paper the hypothesis that recent changes in land use have been large enough to cause the observed drought is tested. Results from a detailed land use model are used to generate realistic maps of vegetation changes linked to land use. The land use model suggests that cropland coverage in the Sahel has risen from 5% to 14% in the 35 yr prior to 1996. It is estimated that this process of agricultural extensification, coupled with deforestation and other land use changes, translates to a conversion of 4% of the land from tree cover to bare soil over this period. The model predicts further changes in the composition of the land surface by 2015 based on changes in human population (rural and urban), livestock population, rainfall, cereals imports, and farming systems.

The impact of land use change on Sahelian climate is assessed using a GCM, forced by the estimates of land use in 1961, 1996, and 2015. Relative to 1961 conditions, simulated rainfall decreases by 4.6% (1996) and 8.7% (2015). The decreases are closely linked to a later onset of the wet season core during July. Once the wet season is well developed, however, the sensitivity of total rainfall to the land surface is greatly reduced, and depends on the sensitivity of synoptic disturbances to the land surface. The results suggest that while the climate of the region is rather sensitive to small changes in albedo and leaf area index, recent historical land use changes are not large enough to have been the principal cause of the Sahel drought. However, the climatic impacts of land use change in the region are likely to increase rapidly in the coming years.

1. Introduction

The African Sahel is a region which exhibits pronounced interannual rainfall variability (Nicholson 1989). However, the drought that has afflicted the Sahel since the late 1960s is without precedent in the modern observational record (Fig. 1). Several mechanisms to account for the prolonged and intense nature of the drought have been proposed. A number of authors (e.g., Lamb 1978; Folland et al. 1986; Fontaine and Janicot 1996) have found links between observed sea surface temperature (SST) patterns in the tropical Atlantic and Pacific Oceans and West African rainfall anomalies. Rowell et al. (1995) were able to reproduce with some success many features of the rainfall time series shown in Fig. 1 by forcing a general circulation model (GCM) with global SST patterns from selected years. Despite the inability of many other models to reproduce this result (Sud and Lau 1996), the overwhelming body of evidence points to a strong influence from SST patterns on rainfall in the region.

Another school of thought has focused on the role of

Corresponding author address: Dr. Christopher M. Taylor, Centre for Ecology and Hydrology, Maclean Building, Crowmarsh Gifford, Wallingford, Oxfordshire 0X10 8BB, United Kingdom.
E-mail: cmt@ceh.ac.uk

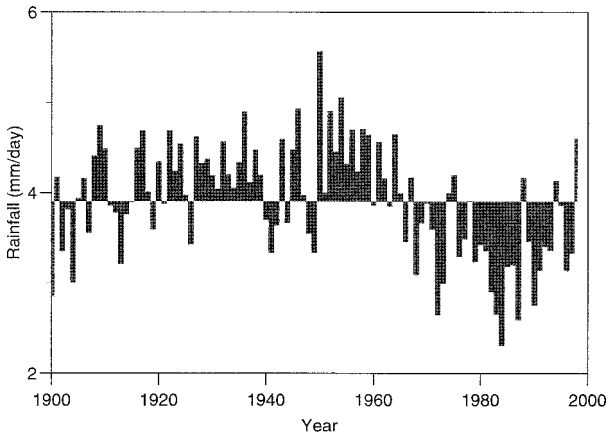

FIG. 1. Observed Sahel rainfall (mm day^{-1}) during the twentieth century (Hulme 1992). The data are averaged over the months Jul–Sep and within 16.88°W and 39.38°E lon, and 11.25° to 18.75°N lat.

land–atmosphere feedbacks. Charney (1975) proposed that rainfall over North Africa is closely linked to the albedo of the underlying surface. He argued that the contrast in albedo between bare soil and vegetation is such that by removing vegetation over the region, atmospheric subsidence would increase, and thereby reduce rainfall. This provides a positive feedback loop, as the drier conditions cannot sustain the return of vegetation. A number of recent studies have examined the functioning of this feedback in the context of ecosystem dynamics. In a study based on a zonally symmetric atmospheric model coupled to an interactive vegetation model, Wang and Eltahir (2000b) were able to simulate both wet and dry equilibrium states over West Africa, associated with contrasting vegetation distributions. They propose that the response of the Sahelian grassland to a reduction in rainfall prolongs the impact of the initial perturbation, leading to lengthy and intense droughts (Wang and Eltahir 2000a). Zeng et al. (1999) similarly argue that vegetation interaction may enhance the interdecadal climate variability in the region, while Claussen et al. (1999) highlight the importance of vegetation feedbacks in the transition from a ''green'' Sahara to its current state during the mid-Holocene period.

A related and much debated mechanism for the drought is the suggestion that its causes are rooted in anthropogenic changes in vegetation. From the numerous GCM experiments where the sensitivity to vegetation cover has been explored, there is a general tendency for rainfall and evaporation to decrease with increasing degradation of the vegetation (e.g., Garratt 1993). Early sensitivity studies in the Sahel (Charney et al. 1977) assumed idealized changes in surface properties, such as an increase in albedo from 0.14 to 0.35, and used a rather simple surface–atmosphere exchange scheme. More recent studies (Xue and Shukla 1993; Xue 1997; Clark et al. 2001), on the other hand, have used a sophisticated surface scheme to represent degradation by the replacement of savannah with bare soil and shrubs. In these experiments, reductions in Sahelian rainfall comparable to those in the recent observational record were reported. Zheng and Eltahir (1997) reported a modest sensitivity of the West African monsoon to desertification in the Sahel, but suggested that regional rainfall may be more sensitive to deforestation further south on the Guinea coast. Finally, Hoffmann and Jackson (2000) suggest that replacing the existing tropical savannah of North Africa with grassland has very little effect on rainfall.

The extent to which land degradation has occurred is not known. Processes such as overgrazing, agricultural expansion, and increased fuelwood extraction have certainly affected the vegetation of the region, with well-documented cases of local degradation (Mabbutt and Floret 1980; Lambin and Ehrlich 1997; Lindqvist and Tengberg 1993). On the other hand, the above modeling studies have examined the effect on climate of wide-scale degradation across the entire Sahelian region (or subregions in the case of Clark et al. 2001) with increases in albedo of approximately 0.08. There is no observational evidence to support such a change in albedo across the region (Gornitz 1985; Nicholson et al. 1998). Unfortunately, satellite observations do not date back to the period before the drought. However, examination of the Advanced Very High Resolution Radiometer (AVHRR) record over the past 20 years suggest that there is no regional-scale evidence of advancing desertification (Prince et al. 1998). Instead the vegetation cover, as quantified by the normalized difference vegetation index (NDVI), shows marked interannual variability largely in step with rainfall anomalies.

Exaggerated changes in land cover were used in the previously mentioned degradation modeling studies in order to increase the statistical significance of the result (Xue 1997). It remains important, however, to establish just how much anthropogenic vegetation changes have contributed to the drought in recent decades. This question becomes even more relevant when considering the future climate. Changes in vegetation are closely linked to human population, technology, markets, and policies. Population in the region is currently doubling every 20 yr and the Sahelian countries are increasingly interconnected with the rest of the world. This paper therefore attempts to quantify the effects of land use change in the last 30 yr on the climate of the western and central Sahel. The climate in this region has been highlighted by Clark et al. (2001) as being particularly sensitive to degradation. We also attempt to predict the impact of future land use change on climate in the region. In order to answer these questions, we first present a detailed land use model designed specifically for the Sahel (section 2). The results of this model are then converted into vegetation parameters within the land surface scheme of a GCM (section 3). The GCM is run, forced by estimates of vegetation for three periods: at the beginning of the 1960s, in the mid-1990s, and finally for 2015 (section 4). Differences between the runs then pro-

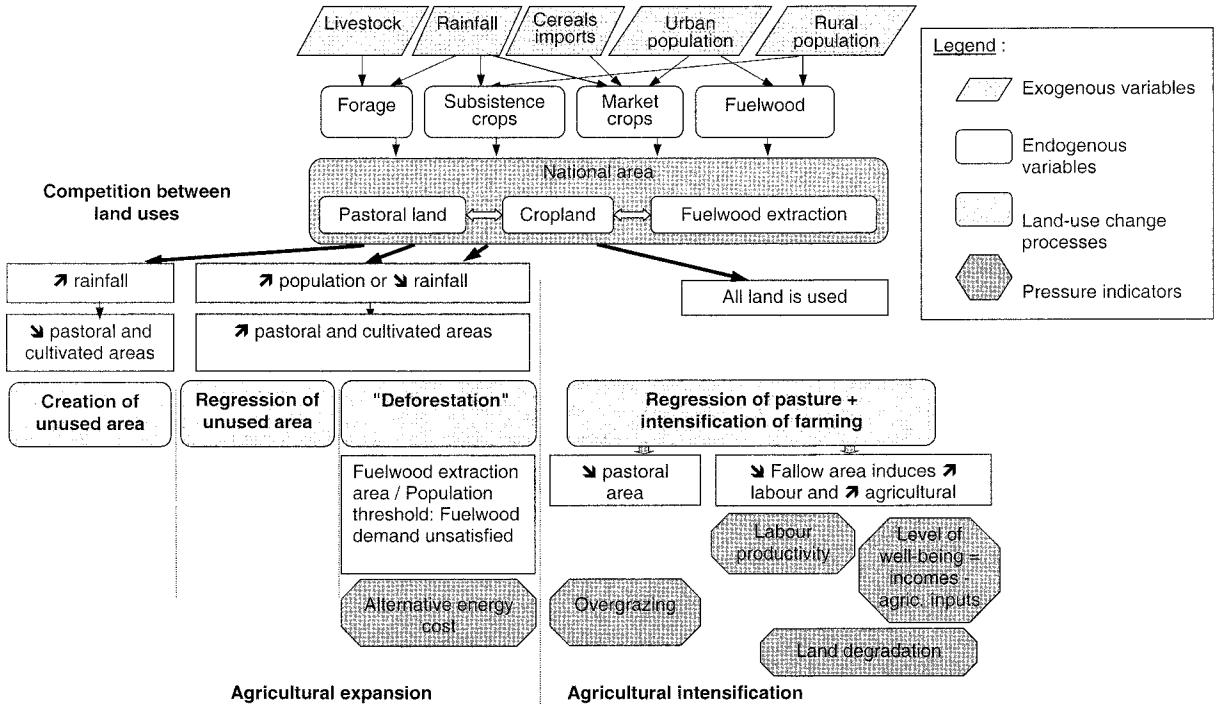

FIG. 2. Overall structure of the SALU model.

vide an estimate of the effects of land use change on past and future climate.

2. Land use change

Past land-cover changes in the Sudano–Sahelian region were reconstructed based on backward projections with the Sahelian land use model (SALU; Stephenne and Lambin 2001a). SALU is a dynamic simulation model designed to represent regional-scale land use change processes in the African Sahel over a timescale of around 30 yr backward and forward. Five land uses generate the basic resources for the population: fuelwood in natural vegetation areas, food for subsistence and market needs in cropland and fallow, and livestock in pastoral land. These land use categories do not strictly coincide with land cover types; for example, the fuelwood extraction area and pastoral lands correspond to vegetation cover types such as woodlands, savannahs, or steppes. The exogenous variables (rural and urban human population, livestock population, rainfall, and cereals imports) drive yearly changes in land use allocation. For any given year, the land use demand is calculated under the assumption of an equilibrium between the production and consumption of resources. Thus, the supply of food and energy resources derived from the areas allocated to the different land uses must satisfy the demand for these resources by the human and animal populations, given the exploitation technologies used at a given time.

In the model, fuelwood extraction areas, cropland, fallow and pastoral land compete for land through different processes of land use change (Fig. 2). The total demand for land in a given year is the sum of demands for cropland and pastoral land. The fuelwood extraction area can be reduced on an annual basis by the expansion of cropland and pastoral land. Within the pastoral land, consumption of forage equals biomass production. For areas under cultivation, both food crops for the rural population and crops for the market are taken into account. The demand for subsistence food crops depends on the rural population and its basic consumption requirements. The crops that are commercialized consist mainly of food crops for the urban population, but also include cash crops (e.g., cotton). Cereal imports are only directed toward the urban population. Finally, the model assumes that at the most extensive level of cultivation, the crop–fallow cycle is 2 yr of fallow for 1 yr of cultivation.

The model simulates two processes of land use change: agricultural expansion at the most extensive technological level, followed by agricultural intensification once a land threshold is reached. Expansion of cropland and pastoral land is driven by changes in human and animal populations, which increase the consumption demand for food crops and forage, and interannual variability in rainfall, which modifies land productivity and therefore increases or decreases production for a given area under a pastoral or cultivation use. Expansion of cultivation can take place into previously uncultivated areas or by migration into unsettled areas. Agricultural expansion thus leads to deforestation or to

a regression of pastoral land. Pastoral land can also expand into natural vegetation areas and cropland. The unused land only becomes reforested after it is left unused for a period of 20 yr. Not all natural vegetation areas can be destroyed. The local population always protects a certain fuelwood extraction area to satisfy some of its fuelwood requirements for domestic consumption, or as forest reserves, national parks, sacred forests, inaccessible forests, or forests with a high risk of diseases. If fuelwood needs exceed the wood production through natural regrowth of vegetation, rural households turn to other energy sources such as kerosene.

Once the expansion of cropland and pastoral land has occupied all unused land, and when fuelwood extraction areas have reached their minimal area, additional demand for food crops mainly results in agricultural intensification and, to a lesser extent, the expansion of cultivation in pastoral land. Intensification mostly takes place as a shortening of fallow cycle, compensated by the use of labor and agricultural inputs to maintain soil fertility. If the crop–fallow cycle is shortened without inputs, then soil fertility is depleted. Should the livestock population increase in combination with shrinking pastoral lands (due to agricultural expansion), overgrazing results, thus affecting the productivity of pastoral land. A more detailed presentation of the model is given in Stephenne and Lambin (2001a).

The model includes 21 parameters for which values were defined from an extensive review of the literature on the Sudano–Sahelian region. A sensitivity analysis shows that, when varying the parameter values by $\pm 10\%$, a variation of no more than 10% in the rate of annual land use changes is found, except for the carrying capacity and food consumption. Values of the exogenous variables of the model were extracted for every year from the Food and Agriculture Organization of the United Nations (FAOSTAT; FAO 1995) and West African Long Term Perspective Study (WALTPS; Brunner et al. 1995) databases, and from the global monthy precipitation dataset gridded at 2.5° latitude × 3.75° longitude resolution (Hulme 1992).

The model was first tested at a national scale using data from Burkina Faso, over the period 1960–97 (Stephenne and Lambin 2001a). The annual rates of change in cropland predicted by the model simulations for Burkina Faso were similar to rates measured for local-scale studies by remote sensing: around 5% in the expansion phase (1960s to early 1980s) and 1.5% in the intensification phase (mid-1980s to 1990s) (Lindqvist and Tengberg 1993). The application of the model to five other countries (Senegal, Mali, Niger, Chad, and Nigeria) also demonstrated the robustness of the approach (Stephenne and Lambin 2001b). For Chad and Mali, land use projections were disaggregated per eco-climatic zone (e.g., mostly pastoral Sahelian zone versus Sudanian zone dominated by farming). The regional-scale projections generated by the model were compared to the International Geosphere–Biosphere Programme Data and Information Services (IGBP-DIS) land cover map of 1992/93, produced from 1-km-resolution remote sensing data (Loveland et al. 1999). A very good agreement between the two sources was found when applying the most favorable correspondence between the SALU land use classes and IGBP-DIScover land cover classes (Stephenne and Lambin 2001b). To generate regional-scale projections of land use changes, the results of SALU-based projections were represented at the resolution of the grid boxes used by the GCM, on the basis of the proportion of each grid box covered by each administrative unit used by SALU.

TABLE 1. Land use (%) in the study area as estimated by SALU for 1961, 1996, and 2015. The study area comprises Senegal, Niger, Chad, Mali, Burkina Faso, and northern Nigeria.

	1961	1996	2015
Fuelwood	72	40	35
Pasture	14	16	17
Cropland	5	14	22
Fallow	9	16	15
Unused	0	13	11

All regions display two time frequencies of land use changes: high frequency, as driven by interannual rainfall variability, and low frequency, as driven by demographic trends and farming system changes. Over the 1961–96 period, the model simulations reveal that agricultural intensification appears sooner in some parts of the Sudano–Sahelian region (Senegal, northern Nigeria, and Burkina Faso) than in others. In 1961, the region was mostly dominated by fuelwood extraction areas and unused land while, starting in the 1990s, greater regional differences in land use distributions are visible. In the entire Sahelian region and in the Sudanian part of Chad, Mali, and Burkina Faso, pastoral land, cropland, and fallows have generally increased while fuelwood extraction areas have shrunk. Elsewhere, and in particular in northern Nigeria, croplands have increased sharply at the expense of savannahs at the end of the 1980s (Stephenne and Lambin 2001b). The results for 1961, 1996, and 2015 are presented in Table 1, based on the averaging by area of results from the separate countries.

3. Representing land use change in the GCM

The GCM used in this study is the U.K. Met Office Hadley Centre Unified Model, which is configured with a horizontal resolution of 2.5° latitude × 3.75° longitude, and 30 levels in the vertical. The model (version HadAM3) contains a suite of physical parameterizations (e.g., radiation, convection, etc.), which are described more fully by Pope et al. (2000) and references therein. Of particular relevance to this work is the land surface scheme, and how we modify it to represent land use change.

a. Mapping land use onto vegetation classes

Land–atmosphere fluxes are calculated in the model by the Met Office Surface Exchange Scheme (MOSES2; Essery et al. 2002, manuscript submitted to *J. Hydrometeor.*, hereafter EBBCT). The scheme requires maps of the fractional coverage of basic land surface components, such as trees and bare soil, at the horizontal resolution of the model. It is, therefore, necessary to interprete the land use classes provided by SALU in terms of MOSES classes. Furthermore, the mapping must reflect the differences in composition of land use classes under varying climatic conditions, notably the sharp rainfall gradient across the Sahel.

For the region under study, the relevant MOSES classes are broadleaf trees, shrubs, C4 species (grasses and crops), and bare soil. We assume that each land use class is made up of a combination of the four MOSES classes, the proportions of which depend on long-term rainfall conditions. The relationships between land use and MOSES classes are presented in Fig. 3, based on values from the literature described next.

Firstly, we assume that the composition of fuelwood extraction areas resembles the natural open canopy forest of the region. Bremen and Kessler (1995) suggest a simple linear relationship between woody cover in forest and rainfall under favorable soil, topographic, and nondrought conditions. We assume the woody cover is predominantly trees, with the remaining area covered by grasses and, under increasingly dry conditions, bare soil. Le Houérou (1989) suggests typically 20% grass cover for pristine vegetation in the 100–200-mm annual rainfall zone.

Cropland areas are assumed to have been cleared of shrubs, with only a few useful trees remaining. D'Herbès and Valentin (1997) suggest typically 5% woody cover in fields within the Hydrological Atmospheric Pilot Experiment (HAPEX)-Sahel study area in southwest Niger (mean annual rainfall 500–600 mm; Goutorbe et al. 1994), while Olsson (1985) reports 6% tree cover in the 300–600-mm zone of Sudan. Tree cover in agricultural areas increases in wetter conditions, Bremen and Kessler quoting typical parkland tree coverage of 0%–10% in the 150–600-mm zone and 5%–20% in the 600–1200-mm zone. The coverage of the MOSES grass type in the remaining area of the fields is not complete. D'Herbès and Valentin reported between 15% and 50% coverage from fields within the HAPEX square depending on, among other things, soil moisture conditions. Given the importance of adequate soil moisture, crop coverage is assumed to decrease with diminishing mean annual rainfall conditions.

The composition of fallow lands in the region changes over time as shrubs redevelop on cleared land. D'Herbès and Valentin suggest total woody cover in young fallow (less than 3 yr) of 5%, with values ranging from 10% to 50% in old fallow (over 7 yr). Bremen and Kessler report that woody cover regeneration in the wetter conditions of the Sudan is more rapid, depending on grazing pressure. D'Herbes and Valentin suggest that typically 20% of fallow land (old and new) in the HAPEX square is bare soil, with a herbaceous understory redeveloping rapidly when a field is unused. The percentage of bare soil is likely to rise with decreasing soil moisture. In this work, the composition of the SALU class ''fallow'' is taken from literature values for older fallowlands of at least 3 yr. The composition of unused land in SALU, formerly crop or pasture, is considered here to be similar to that of young fallow.

Relative to natural forests, pastoral lands tend to have a low woody coverage. This is due to the burning and removal of shrubs. Moderate grazing in pastoral land can stimulate productivity of the remaining vegetation (Bremen and Kessler 1995). Grass cover is therefore quite high for the pasture class, as we assume that overgrazed areas are rather localized, and do not affect the entire region.

Over the study area, gridded fractional coverages of the MOSES classes are produced using the land use conversions (Fig. 3), the observed rainfall climatology (Hulme 1992), and the national results from SALU, mapped onto the Unified Model (UM) grid. Figure 4 shows the coverage of two MOSES classes in 1996 and 2015, as compared to the coverage in 1961. By 1996, 3.9% of the area loses tree cover, accompanied by a 4.2% increase in bare soil. These changes increase to 4.8% and 5.7%, respectively, by 2015. Loss of tree cover is greatest in southern Mali, while crop expansion in northern Nigeria and Senegal accounts for the areas with the largest increase in bare soil. In the northern Sahel on the other hand, changes in the coverage of MOSES classes are strongly constrained by the low rainfall and associated very sparse vegetation cover.

b. The land surface model

The land surface model used in this study (MOSES2) is an extension of the original Met Office Surface Exchange Scheme (Cox et al. 1999). MOSES includes a model for plant photosynthesis and stomatal conductance, evaporation from canopy water, bare soil and transpiration, and a four-level soil scheme for the transfer of heat and water. The principal advance in MOSES2 is in the treatment of subgrid heterogeneity; instead of using average parameters to calculate a single energy balance, a separate surface energy balance is calculated for each functional type in a grid box. The heat and moisture fluxes into the atmosphere are then the sum of the individual fluxes weighted by their fractional coverage. Outside of the study area, fractional coverages are derived from the IGBP DIS land cover map (Loveland et al. 1999).

A number of changes are made to the standard set of parameters associated with the vegetation classes in the Sahel. A seasonally varying leaf area index (LAI) is introduced for each grid point and each plant functional

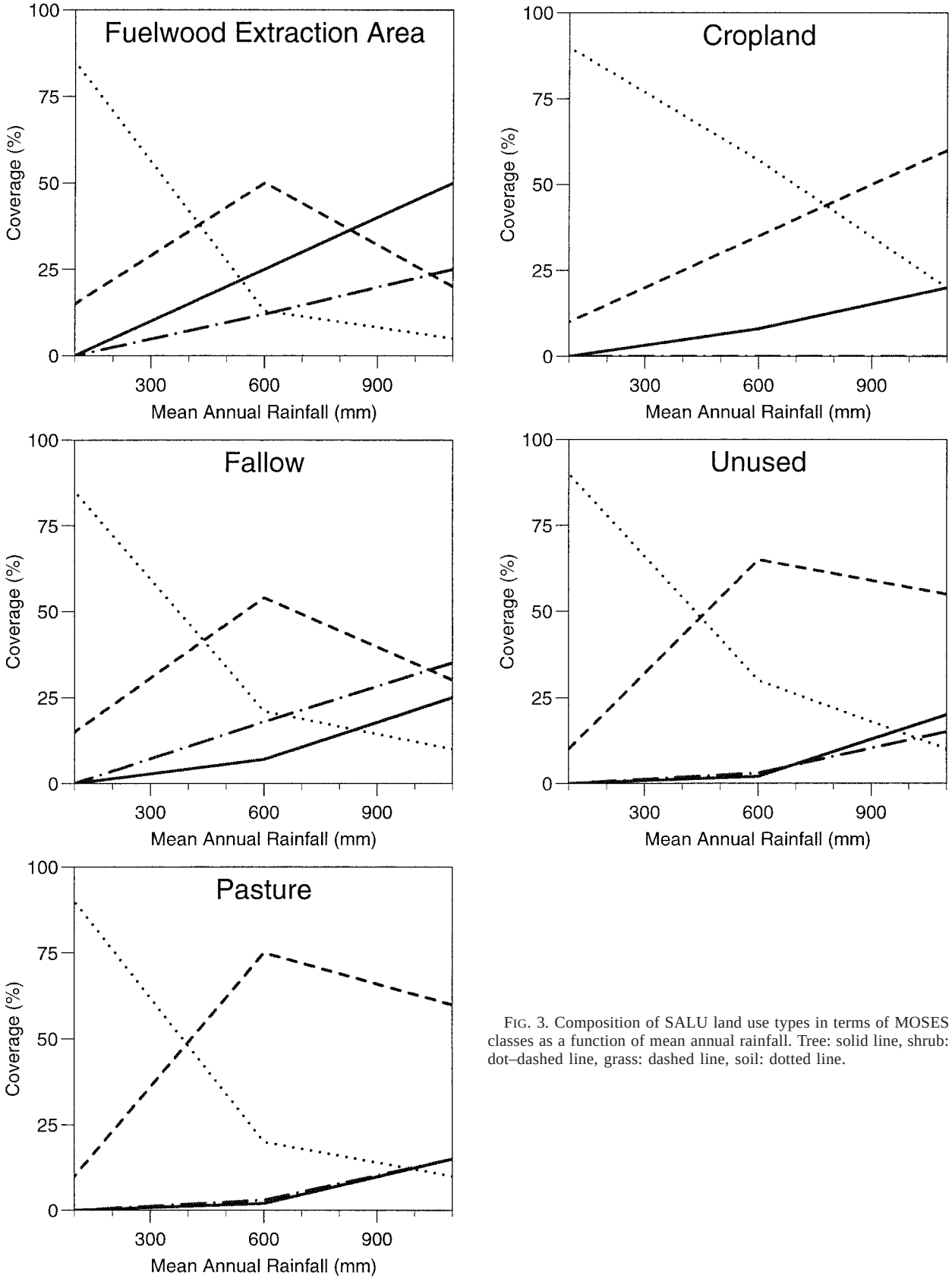

FIG. 3. Composition of SALU land use types in terms of MOSES classes as a function of mean annual rainfall. Tree: solid line, shrub: dot–dashed line, grass: dashed line, soil: dotted line.

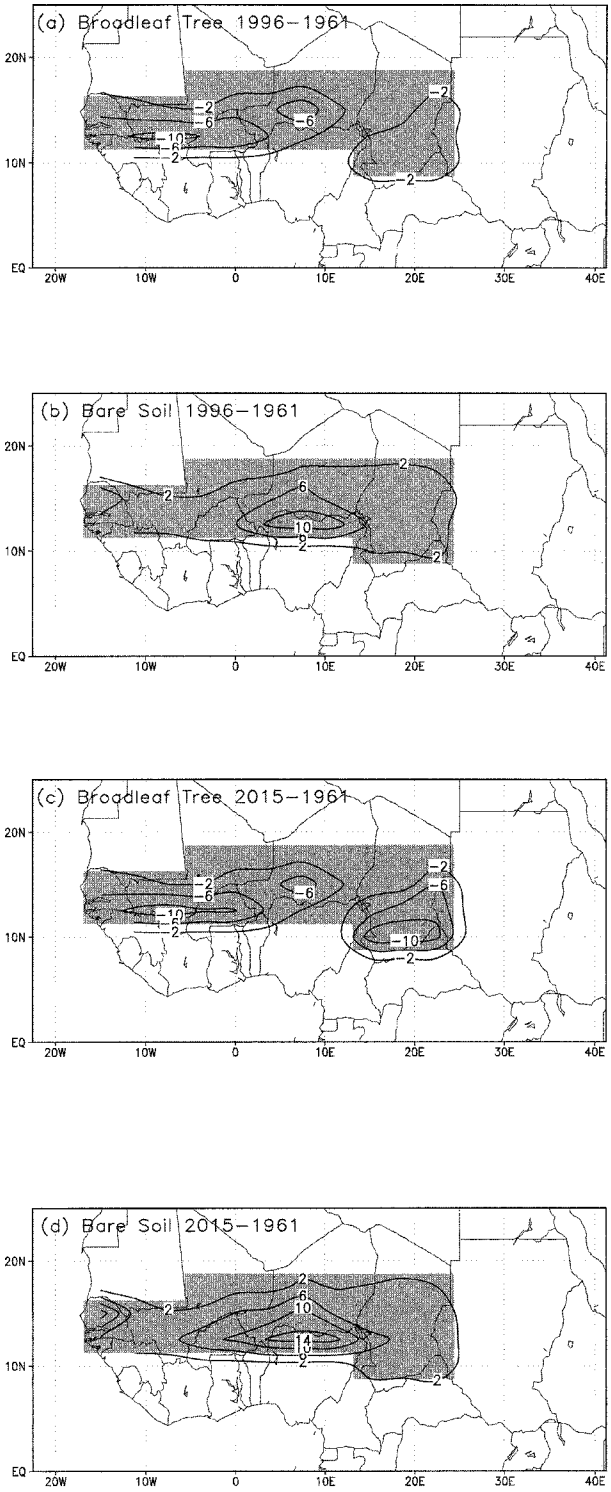

FIG. 4. Changes in coverage (%) of (a), (c) broadleaf tree and (b), (d) bare soil for 1961–1996 and 1961–2015.

type in tropical North Africa. The LAI in month k is calculated offline from the climatological monthly rainfall R in that area;

$$\mathrm{LAI}(k) = \mathrm{LAI}_{\min} + \frac{\mathrm{LAI}_{\max} - \mathrm{LAI}_{\min}}{(R^i_{\max} - R^i_{\min})}\left\{\left[\sum_{k-i}^{k} R(k)\right] - R^i_{\min}\right\},$$

where the lag between LAI and rainfall, i, equals 1 month for grass and crops, and 2 months for trees, and shrubs, and $R^i_{\max}$ and $R^i_{\min}$ are the maximum and minimum totals of observed rainfall over i months. Values of the maximum and minimum LAI ($\mathrm{LAI}_{\max}$ and $\mathrm{LAI}_{\min}$) used in the Sahel are given in Table 2 for each of the vegetation types considered here. Several related parameters are calculated online by MOSES2 based on LAI, and seasonal maximum and minimum values are again given in Table 2. Additional parameters within the stomatal conductance and photosynthesis model have been calibrated against observations from the HAPEX-Sahel database (e.g., Hanan and Prince 1997). This ensures that the observed stomatal response to environmental conditions, notably atmospheric humidity deficit and temperature is correctly represented.

A dependency of the bare soil albedo on surface soil moisture is included here. In addition, soil hydraulic parameters are derived from the IGBP-DIS soil data task (Scholes et al. 1995). The parameters provided for the Van Genuchten model are converted to the Brooks and Corey scheme used by MOSES following the method of Lenhard et al. (1989). The calculation of suitable areal mean soil parameters is complex as the equations are nonlinear. For simplicity, we use areally weighted values of the soil parameters in each grid box. The exception to this procedure is the hydraulic conductivity at saturation, k_{sat}. The value of k_{sat} is taken to be that which provides the correct area-weighted drainage at 50% saturation. A final modification to the basic MOSES2 scheme is an enhancement of the drainage flux from the top soil level to the second level. This is to account for the subgrid variability of soil moisture assumed to exist after rain events. Following Taylor and Blyth (2000), the hydraulic conductivity

$$K = K_{\mathrm{sat}}\left(\frac{\theta}{\theta_{\mathrm{sat}}}\right)^{\alpha(2b+3)},$$

where θ_{sat} is the value of volumetric soil moisture (θ) at saturation, and b is an empirically determined exponent. Additional drainage occurs by setting α to a number less than unity. Based on rainfall statistics in the Sahel we set $\alpha = 0.45$.

c. *Impact of land use on surface fluxes simulated by MOSES2*

To illustrate the influence of land use on the water and energy balance, two offline simulations with MO-

TABLE 2. Parameters for vegetation classes in the Sahel. Monthly maximum and minimum values are quoted where appropriate. The albedo for each plant functional type includes a component due to bare soil, which is assumed here to be 0.30. The height (and roughness length) of trees is assumed to be constant throughout the year, but varies with climatological rainfall to give smaller trees in the northern Sahel. The root depth quoted defines an exponential distribution with soil depth.

	LAI		Albedo		Canopy capacity		Roughness length (m)		Root depth (m)
	Min	Max	Min	Max	Min	Max	Min	Max	
Broadleaf tree	0.5	5.0	0.15	0.26	0.53	0.75	0.25–0.75*		3.0
Shrub	0.5	2.5	0.20	0.24	0.25	0.45	0.2		2.0
C4 grass	0.1	1.5	0.18	0.27	0.06	0.13	0.02	0.05	1.0
Crop	0.1	2.0	0.30	0.30	0.06	0.15	0.02	0.15	1.0

SES2 are performed that assume either forest cover (fuelwood extraction area) or crops. The model is forced by 7 months of weather station data from a site in Niger (Monteny et al. 1997). Throughout the simulation, net radiation is higher over the forest (Fig. 5), due to a lower albedo and cooler surface temperatures. Evaporation is also higher over the forest. Prior to the wet season, the trees and shrubs have greater access to deep soil moisture, enabling limited transpiration all year-round (Gaze et al. 1998). During the wet season, cropland evaporation is limited by both reduced net radiation compared to forest, and the extensive soil coverage. Evaporation rates over the bare soil are much lower than over vegetation whenever the surface dries out. Similar contrasts in evaporation to those shown in Fig. 5 were demonstrated by Gash et al. (1997) from observations of fluxes over crops, fallow, and patterned woodland areas.

4. Assessing the sensitivity of Sahelian climate to land use

To examine the impact of Sahelian land use on regional climate, the GCM is run with three alternative vegetation scenarios derived from the land use change projections of the SALU model. In the control run, surface parameters in the study area are determined from 1961 land use. Simulations are also made with 1996 and 2015 land use. Following a 5-yr spinup period, each simulation is run over 10 annual cycles. To isolate the climatic influence of land from changing SST patterns, the same SST boundary conditions are adopted in all three runs. The SST data are climatological monthly means for the years 1951 to 1980 (Bottomley et al. 1990).

The simulation of rainfall and its sensitivity to land use over the region are presented in Fig. 6. During the

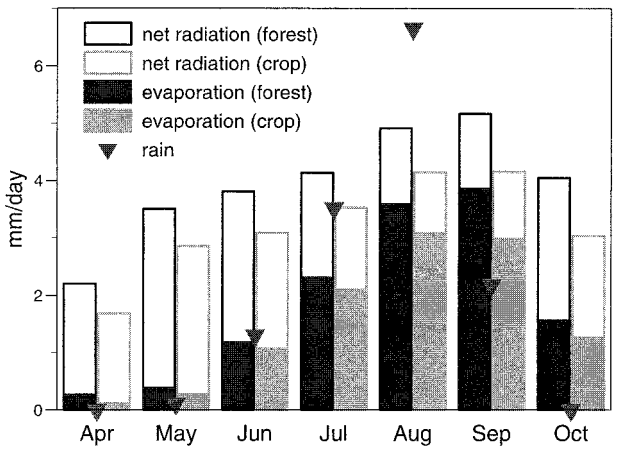

FIG. 5. Offline simulation of net radiation and evaporation (mm day^{-1}) for forest and cropland.

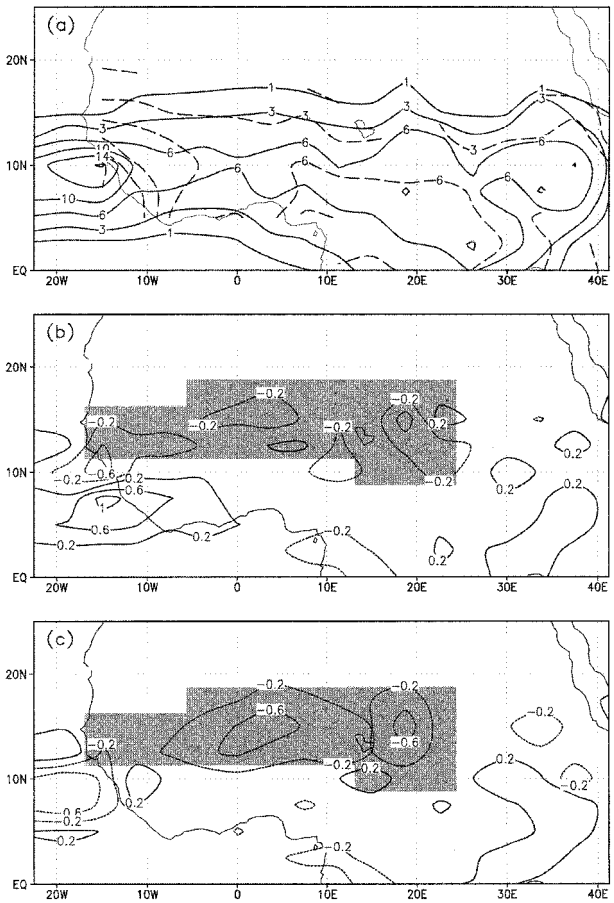

FIG. 6. Mean JAS rainfall (mm day^{-1}). (a) Observations 1900–98 (dashed) and simulated with 1961 land use (solid). (b) Difference between 1961 and 1996 land use. (c) Difference between 1961 and 2015 land use. The area where vegetation changes are applied in (b) and (c) is shaded.

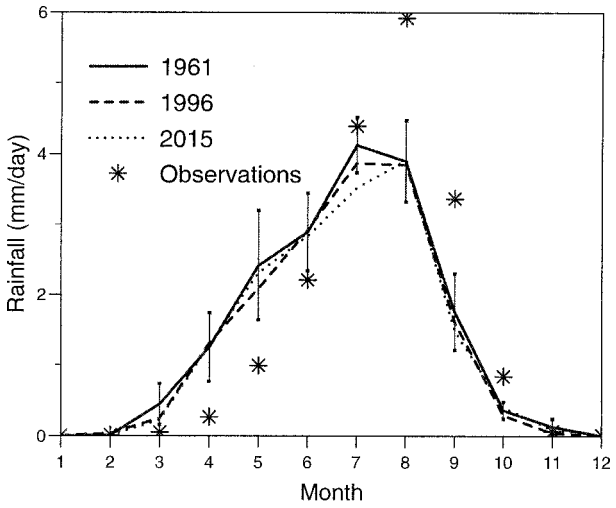

FIG. 7. Monthly rainfall (mm day^{-1}) averaged over the study area for the three land use scenarios. For 1961, the vertical lines indicate the standard deviation of monthly rainfall for the 10 yr. Observations (Hulme 1992) are also shown for reference.

wet season months of July, August, and September (JAS), the model simulates a band of high rainfall spanning the continent. Both the location and latitudinal gradients associated with this band compare well with observations. However, there is a pronounced dry bias in the model near the west coast.

Compared to the 1961 simulations, both 1996 and 2015 land use patterns lead to reductions in rainfall over the vast majority of the study area. Locally, the change in rainfall can exceed 0.8 mm day^{-1} for both 1996 and 2015 land use. The largest changes in rainfall are found in southern Niger and central Chad. Averaged over the entire study area, rainfall decreases from the control value of 3.28 mm day^{-1}, by 0.15 mm day^{-1} (1996) and 0.28 mm day^{-1} (2015). The reduction in rainfall in the 1996 land use simulation are significant at the 95% level (according to a Student's *t* test) for only 5 grid points out of 33 in the study area. This number rises to 11 in the 2015 simulation. Elsewhere, statistically significant increases in rainfall are limited to a region to the southwest of the study area (for 1996 land use only), and also to the southeast in southern Sudan and Ethiopia. Comparison between Figs. 6 and 4 reveals no clear relationship between the location of greatest rainfall reductions and areas of substantial vegetation loss.

a. Annual cycle

The annual cycle of rainfall and surface fluxes in the model are presented as areal averages over the study area in Figs. 7 and 8. The simulation of the annual cycle differs in several respects from observations of rainfall and temperature (not shown). The West African monsoon begins a month too early, bringing excessive rain and overly cool surface conditions during the period April to June. The model does produce a maximum in West African rainfall during August, as observed. However, the band of maximum rainfall does not penetrate as far north as the Sahel, resulting in a substantial dry bias during August and September. Despite these problems, the simulation of the seasonal cycle in this study compares favorably with results using the standard set of surface parameters in both MOSES and MOSES2 (EBBCT). In addition, the surface parameters used here produce a more realistic diurnal cycle of convection (Taylor and Clark 2001).

The sensitivity of rainfall to land use varies during the wet season. There is a substantial rainfall reduction in July with 1996 and 2015 vegetation, in contrast to August when totals are similar. The reasons for this behavior will be discussed in the following section. Interannual variability in monthly rainfall is large in the model (as indicated in Fig. 7), despite the adoption of climatological mean SST patterns. Large interannual variability ensures that the rainfall signal associated with our land use scenarios produces only a low level of statistical significance. With the exception of July for the 2015 scenario, changes in rainfall are smaller than the interannual standard deviation in the control. Although large, the interannual variability simulated by the model in this region is not unrealistic. The JAS mean standard deviation of rainfall equals 0.58 mm day^{-1}, which compares with 0.93 mm day^{-1} in the long-term observations. Adoption of interannually varying SST patterns would increase the model variability further.

The land–atmosphere fluxes shown in Fig. 8 exhibit a clearer sensitivity to land use than does rainfall. Net surface radiation is reduced relative to 1961 throughout the year with both 1996 and 2015 vegetation. The changes are due to a combination of higher albedo and greater longwave loss, and are only partially offset by increased insolation. Evaporation is consistently higher for 1961 land use compared to the other runs. The effect is largest during the wet season and subsequent drydown, and results from a lower evaporative resistance and increased net radiation. Land use change leads to a reduction in sensible heat flux for much of the year, due to a decrease in net radiation. During JAS however, sensible heat flux is greatest for 2015 land use, when the relative availability of soil moisture for evaporation dominates over considerations of available energy.

The atmospheric response to the changes in land surface conditions is largely confined to the planetary boundary layer (PBL), and to within the region of the study area. During JAS, the PBL is a little warmer, deeper, and drier for 2015 (and to a lesser extent, 1996) than in the control run. Interestingly, the changes are smaller during August than in July and September. Notable changes in the wind fields are restricted to July in the 2015 simulation, when there is a relatively large increase in surface heating (Fig. 8). Southerly monsoon flow is enhanced by about 10% in the Sahelian PBL, and the zonal mean African easterly jet (AEJ) is located one grid point (2.5°) further south. Both of these changes

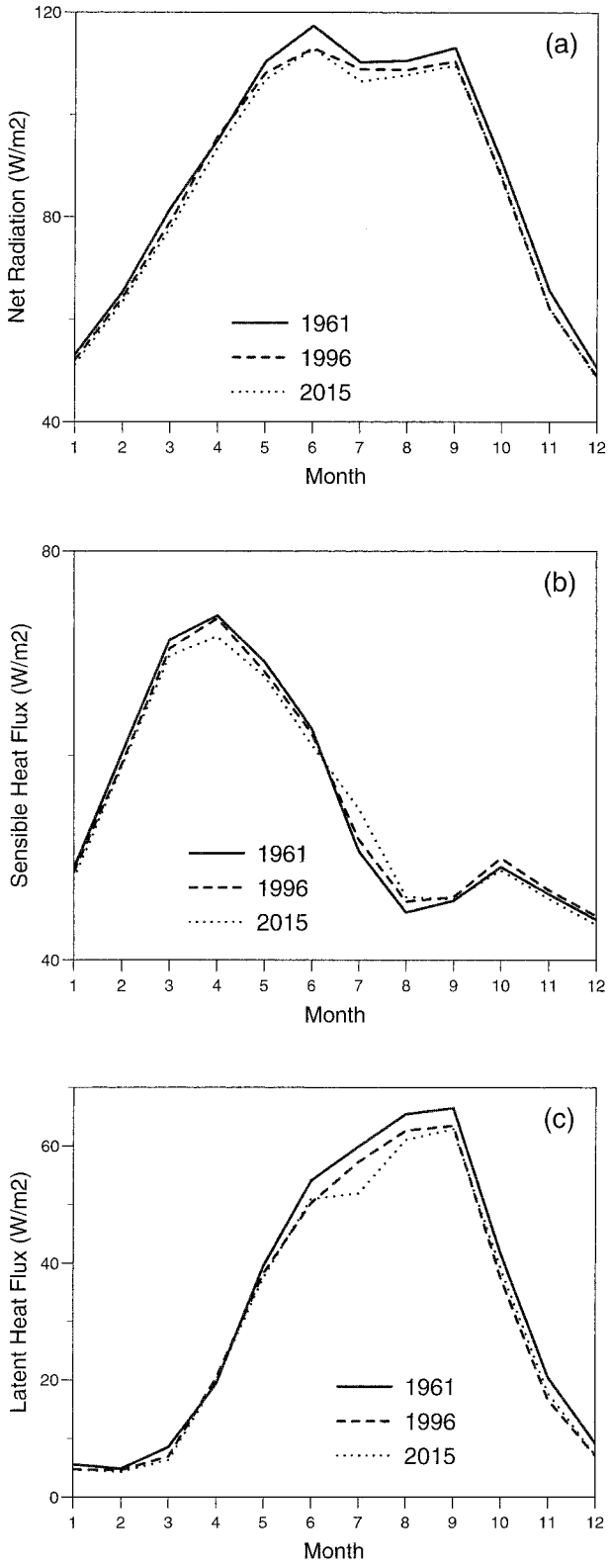

FIG. 8. Monthly mean (a) net radiation (W m^{-2}), (b) sensible heat flux (W m^{-2}), and (c) latent heat flux (W m^{-2}) for the three simulations averaged over the study area.

can be interpreted as a response to the greater surface heat flux contrast between the Sahel and the Sudan to the south.

b. Changes in the core of the wet season

The simulations show a strong reduction in rainfall in July for 1996 and 2015 land use, while August rainfall is relatively insensitive to land use. The evolution of the wet season is illustrated using 10-day means in Fig. 9. In the control run, model rainfall reaches a plateau during July and early August (days 180–220). The onset of this wet season ''core'' is delayed for the alternative land use scenarios by approximately 10 (1996) and 20 (2015) days. This delay accounts for the strong sensitivity of July rainfall to land use (Fig. 7). Once the core of the wet season begins, rainfall accumulations are fairly similar for all three scenarios. Differences in the timing of the end of the very wet period are less clear. Overall there is a shorter wet season core for the later land use scenarios.

Changes in the evaporative fraction (the ratio of latent heat flux to the sum of both sensible and latent heat fluxes) are shown in Fig. 9b. Throughout the year, the evaporative fraction is lower for the later land use scenarios. However, there is a pronounced lag in the rise of evaporative fraction during June and July. This is due to the diminished efficiency of the surface to recycle water (linked to vegetation cover), and is exacerbated by the changes in rainfall when the surface is coupled to the atmosphere. From a simple one-dimensional perspective, higher evaporative fraction can be linked to larger values of PBL equivalent potential temperature (θ_e), and more favorable conditions for deep convection (e.g., Betts and Ball 1998; Eltahir 1998). Figure 9 shows that the lag in evaporative fraction for later land use is indeed accompanied by a lag in θ_e. When the seasonal plateau in θ_e is reached, the system can be considered to be in a ''wet state.'' During this period moist soils maintain high evaporation rates, ensuring a humid and shallow PBL. These conditions favor high rainfall rates, which then feed back on soil moisture, thus maintaining wet conditions. Compared to the 1961 scenario, the wet state is reached about a month later for 2015 land use, with 1996 falling between the two scenarios. The timing of the decline in θ_e is similar in all three runs, although the decline is more rapid for the later land use scenarios.

Rainfall in July exhibits a relatively strong sensitivity to land use because vegetation is important in the development of a wet state. During August on the other hand, the sensitivity to land use is small. Interestingly, previous studies of Sahelian land cover change (Xue and Shukla 1993; Xue 1997; Clark et al. 2001) also show that land degradation has a weaker impact on rainfall during August. To understand the weak sensitivity of rainfall in August to land use in this study, it is instructive to examine rainfall at the event timescale. Intense rainfall events are closely linked to the passage

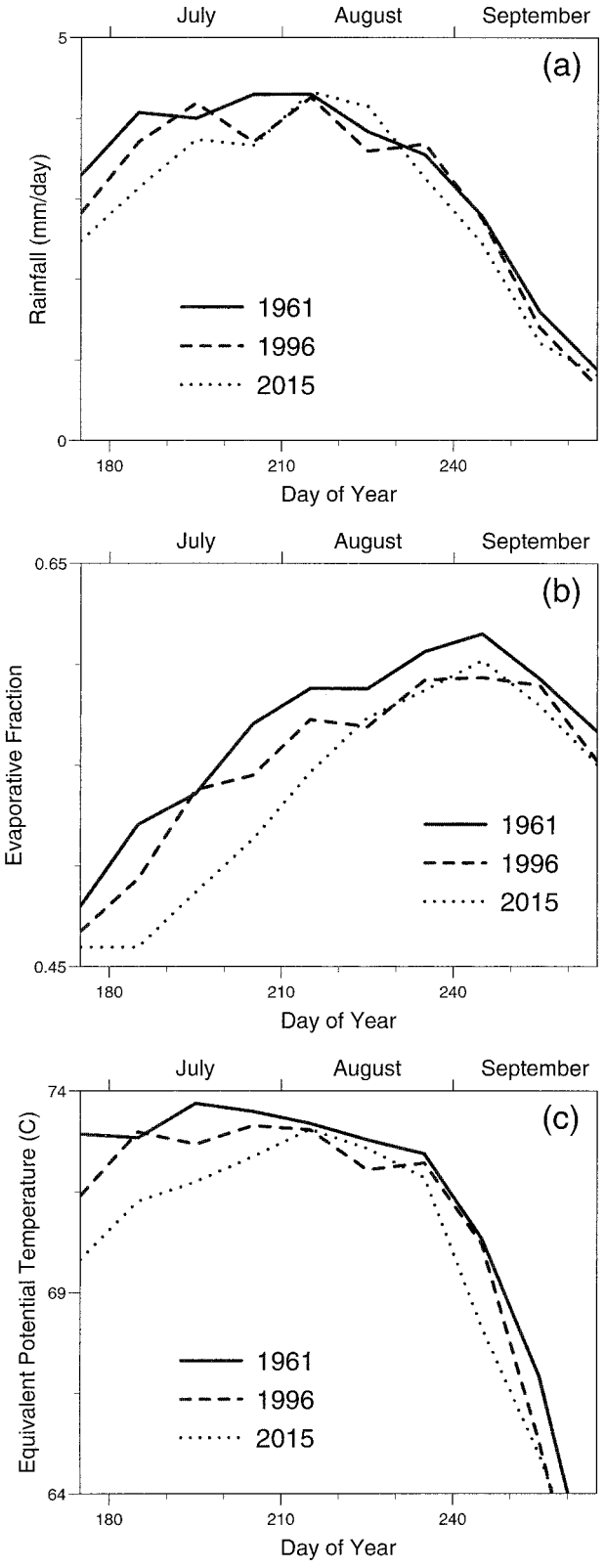

FIG. 9. Wet season 10-day-mean diagnostics averaged over the study area. (a) Rainfall (mm day^{-1}), (b) evaporative fraction, and (c) equivalent potential temperature (θ_e; °C) at the first model level.

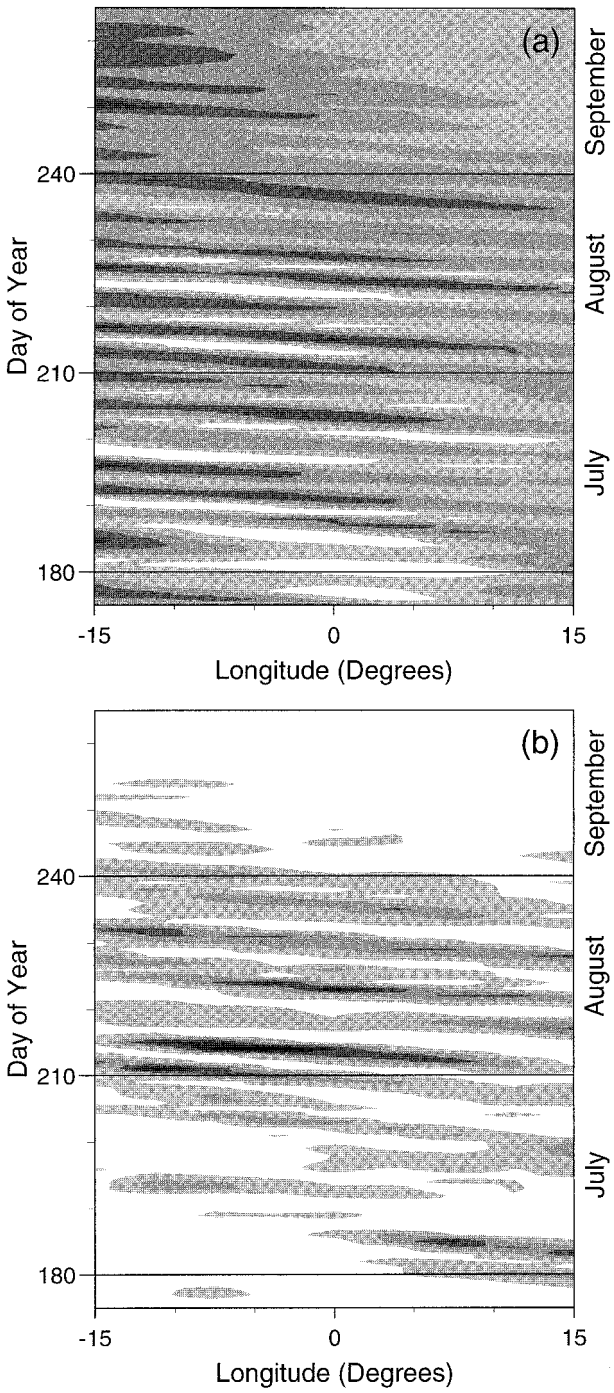

FIG. 10. Hovmoeller plots of (a) 700-hPa meridional wind and (b) rainfall averaged between 11.25° and 18.75°N from a single wet season with 2015 land use. Shaded contours are plotted (a) every 3 m s^{-1} and (b) every 4 mm day^{-1} starting at 2 mm day^{-1}.

of African easterly waves (AEWs) in the model, as illustrated by the Hovmoeller plots in Fig. 10. Figure 10a shows the development of waves (identified here by anomalies in 700-hPa meridional wind) in the central Sahel, and their subsequent westward propagation (e.g.,

TABLE 3. Results from a composite wave analysis between 15°W and 11.25°E at 12.5°N showing the mean number of waves identified at each grid point, the mean rainfall rate over 24 h from the time of passage of the maximum northerly wind, and (in brackets) the rainfall contributed by these events to the monthly mean.

	1961		1996		2015	
	Number of waves (month^{-1})	Rain (mm day^{-1})	Number of waves (month^{-1})	Rain (mm day^{-1})	Number of waves (month^{-1})	Rain (mm day^{-1})
Jul	3.63	11.5 (1.39)	3.49	11.0 (1.28)	4.20	8.6 (1.20)
Aug	4.66	11.2 (1.74)	4.55	11.9 (1.80)	5.04	12.6 (2.12)

Albignat and Reed 1980). In the model, heavy rain events tend to propagate westwards ahead of the wave trough (Taylor and Clark 2001). Frequent passage of these events mark the wet season core.

A wave composite procedure (Taylor and Clark 2001) has been applied to these simulations, with waves identified whenever a northerly wind at 700 hPa deviates from its 4-day running mean value by at least 2 m s^{-1}. Table 3 provides a summary of both the number of AEWs identified, and the mean rainfall intensity associated with propagating storms ahead of the wave trough. Only results from 12.5°N are presented, but similar behavior is found at other latitudes in the study area. Wave activity is greatest during August in the study area for all three simulations. Relative to 1961, there is a 12% increase in the number of waves using 2015 land use. One possible reason for this rise may be the increasing sparseness of the vegetation. Taylor and Clark (2001) found that fluxes from a sparsely vegetated Sahel led to an efficient amplification of low-level thermodynamic properties within an AEW.

The average rainfall intensity of the propagating storms falls slightly between July and August in the 1961 simulation. On the other hand the rain per event rises modestly between July and August for 1996, and more dramatically so in the 2015 simulation. The July decrease and August increase in rain per wave between the 1961 and 2015 simulations are both significant at the 95% level. The reduction of rain per wave in July for 1996 and 2015 land use may be linked to changes in PBL θ_e (Fig. 9). Relatively low values of θ_e during July in the 2015 simulation are likely to limit the intensity of convection associated with the AEW. The reasons for higher values of rain per wave during August for the later land use scenarios are not clear. Finally, combining the frequency and rainfall data in Table 3, the contribution to total rainfall of storms ahead of wave troughs can be estimated. Relative to the control, this contribution for 1996 and 2015 land use is reduced in July. During August, however, the contribution of propagating storms to total rainfall actually increases for the later land use scenarios.

In summary, the contrasting sensitivities of July and August rainfall to land use are linked to two mechanisms. First, more-intensive land use limits the efficiency of the surface to recycle moisture, as found in other studies. During July, this effect produces a delay in the onset of the core of the wet season, hence reducing July rainfall for the 1996 and 2015 scenarios. Second, once the wet season core is established, and AEWs become an important control on convection, the sensitivity of rainfall to land use is also influenced by the impact of the land surface on the characteristics of the synoptic storms. In this experiment during the month of August, AEWs are more numerous and produce more intense rainfall for 2015 land use than in the control. The second mechanism then offsets the first so that total August rainfall is hardly changed. While the first feedback mechanism is relatively well understood, the links between vegetation changes and the frequency and intensity of synoptic storms are less clear. For example, Polcher (1995) found that following tropical deforestation in a series of GCM experiments, the change in regional rainfall was closely associated with the change in frequency of synoptic storms. This characteristic grew with increasing sensible heat flux, producing a counterintuitive increase in rainfall following deforestation in some experiments.

5. Comparison with previous studies and observations

In order to place our conclusions in context, it is interesting to compare the results from this study with previous GCM experiments and observations. Before considering the observations, it is important to note that our simulations assume the same SST conditions for all land use scenarios. The simulations therefore exclude an important contributing factor to the observed changes in rainfall. Second, our scenarios assume no changes in biophysical properties (e.g., LAI) for any particular land use class, and simply reflect a change in fractional coverage of that class. In reality, during dry years the seasonal development of vegetation is restricted strongly by moisture stress. Since the 1960s, rainfall conditions have been generally poor, and this would have produced a loss of vegetation cover by biophysical feedbacks even without changes in land use. Therefore the vegetation loss assumed here is an underestimate of the actual decrease of vegetation cover.

Changes in rainfall and key land surface properties averaged over the study area are presented in Table 4 for the two land use change scenarios. Also in Table 4 are results from a previous study (Xue 1997, hereafter X97) using the Center for Ocean–Land–Atmosphere studies (COLA) GCM. In that study, the changes in

TABLE 4. Changes in surface properties and the total percentage change in rainfall from the two land use change scenarios, a previous study, and observations, where available. The changes are averages over JAS.

	Rainfall (%)	Albedo (×100)	Roughness length (cm)	Bare soil fraction (×100)	LAI
1996 − 1961	−4.6	+0.54	−2.3	+4.2	−0.13
2015 − 1961	−8.7	+0.88	−2.9	+5.7	−0.16
Xue (1997)	−34	+8.5	−55.	+10.	−2.2
Observations	−20 (1948–67 vs 1968–97)	Unknown (interannual variability ± 2–3)	Unknown	Unknown	Unknown (interannual variability of NDVI ~ 0.5)

vegetation are more idealized, reflecting large-scale land degradation throughout the Sahel and Sudan. The intensity of land cover change in X97 is similar to other studies (Xue and Shukla 1993; Clark et al. 2001).

We estimate that the impact of land use change alone between the early 1960s and mid-1990s led to an increase in albedo at the regional scale of 0.0054. This change is well within the range of both observed interannual variability and instrumental error (Nicholson et al. 1998). As discussed above, it is likely to be an underestimate of the actual increase in albedo during those decades as it excludes important ecological processes. On the other hand, our estimated albedo change is a factor of 15 smaller than that adopted by X97. In that study, it is noted that an increase in albedo of 0.085 is ''exaggerated to obtain more statistically significant results.'' There is controversy as to whether such a large albedo change at the regional scale may have occurred in recent decades (Nicholson et al. 1998). Here, we simply note (in agreement with Gornitz 1985) that from land use considerations alone the albedo changes adopted in previous studies are unrealistic. Similarly, compared to our estimates, prescribed changes in LAI and roughness length in X97 are also an order of magnitude larger. As with albedo, our LAI change under both scenarios is probably smaller than that associated with natural interannual variability, based on NDVI observations since 1981 (Goward and Prince 1995). Finally, our estimated increase in bare soil fraction is only a factor of 2 smaller than that used in X97. In all of these comparisons, however, it is worth bearing in mind that X97 used a different land surface scheme Simplified Simple Biosphere model (SSiB; Xue et al. 1991) from that used here, and the selected parameters are likely to function differently within the two schemes.

Simulated rainfall (JAS mean) is reduced by 4.6% when 1961 vegetation is replaced by 1996 vegetation. The rainfall reduction is nearly doubled when considering the expected vegetation changes in the subsequent 20 yr to 2015. Both the sign of the rainfall change, and its sensitivity to the intensity of vegetation change are consistent with many previous studies (e.g., X97). Unlike a number of these studies, however, our vegetation changes do not produce rainfall reductions comparable to those observed since the end of the 1960s. It is probable that this result is due to the relatively modest changes in vegetation that we prescribe. The vegetation changes are consistent with recent scientific findings that show that land degradation in the African Sahel is localized (e.g., Prince et al. 1998), that semiarid ecosystems are resilient to grazing pressures (e.g., Lambin et al. 2001), and that the case of desertification in the African Sahel has been overstated in the literature and in global datasets (Fairhead and Leach 1996).

It is possible that the changes in rainfall in this study are rather small compared to those in X97 because the experiments were performed using different GCMs. Clark (1999) undertook a comprehensive comparison of the Unified Model and the COLA GCM (as used in X97), and in particular, their sensitivity to vegetation changes. He applied very similar Sahelian desertification scenarios in both models, and found that after desertification, there was a 34% decrease in rainfall in the Unified Model, compared to 32% in the COLA GCM. The similar response of the two models in this case suggests that the weaker rainfall signal in the current study is indeed due to smaller changes in surface properties than were adopted in X97.

6. Conclusions

This paper presents an attempt to quantify the impact of land use changes on climate in the Sahel, and in particular, to examine the hypothesis that anthropogenic changes to the land surface caused the drought conditions that have persisted since the late 1960s. In the absence of regional-scale observations of vegetation cover dating back before the drought, we have generated land cover scenarios for a GCM based on the results of a detailed land use model. Averaged over the six countries considered in the Sahelian belt of West Africa, the land use model estimates that the fraction of land used for crops increased from 5% in the early 1960s to 14% by the mid-1990s, accompanied by a loss of natural forest cover of 28%. These changes are thought to be realistic and are consistent with observational results from local-scale studies of land use change in the Sahel. Assuming larger rates of cropland expansion or land degradation at the scale of the entire region would be counter to all empirical evidence collected by remote sensing and field observations. The latter two sources

only reveal the presence of localized land degradation in areas subject to considerable and permanent stress.

Wet season rainfall simulated by the GCM is reduced by 4.6% when estimates of land use from 1996 are used to prescribe vegetation characteristics, rather than those from 1961. The reduction of rainfall reaches 8.7% when land use projections for 2015 are adopted. Diminished rainfall with later land use is associated with the delayed onset of the wet season core during July. Once established, however, rainfall rates at the height of the wet season are relatively insensitive to land use. Compared to an observed rainfall reduction in recent decades of 20% over the region, it seems reasonable to conclude that land use changes have not been large enough to have caused the persistently low rainfall observed. Regional and global SST patterns are a more likely candidate. However, it should not be assumed that land–atmosphere feedbacks have played no role in the drought. On the contrary, the sensitivity of regional rainfall in this study to albedo changes of less than 0.01 imply that the climate system in the Sahel is very sensitive to land surface conditions. Purely through biophysical feedbacks, interannual rainfall variability in the region provides changes in albedo and LAI rather larger than those imposed here. However, such processes have not been considered here, in order to isolate the anthropogenic processes. These facts suggest that natural vegetation variability in the region is also likely to have played an important role in the recent drought, in agreement with several recent studies (e.g., Wang and Eltahir 2000a; Zeng et al. 1999). They suggest that ecosystem dynamics may prolong externally forced drought conditions. Examining the role of vegetation dynamics on climate variability is clearly an important avenue for future investigations, and one which may also be of relevance to other regions of the world.

The results from the land use model imply that the loss of vegetation cover is likely to continue, driven by a rapidly growing population and provided that no major change in land use policies and attitude is taking place. Based both on previous work and the GCM results presented here, the impact of land use on rainfall is therefore likely to increase. A further potential feedback loop emerges as land use is itself very sensitive to rainfall. Any prolonged droughts in the coming years will trigger further deforestation, agricultural extensification and modification in pastoral land use, potentially leading to more conflicts between pastoralists and farmers. Coupled to the natural climate-forced variability of vegetation and the pronounced regional climate impacts of SST anomalies, these anthropogenic effects may contribute to a further decrease in the stability of Sahel rainfall, and therefore in the stability of Sahelian societies as a whole.

Acknowledgments. The authors would like to thank Doug Clark, Eleanor Blyth, and the reviewers for their comments on this work. The work was partly funded by the European Union Contract ENV4-CT98-0696. The development of MOSES was supported by the UK DEFRA Climate Prediction Programme under Contract PECD 7/12/37.

REFERENCES

Albignat, J. P., and R. J. Reed, 1980: The origin of African wave disturbances during phase III of GATE. *Mon. Wea. Rev.,* **108,** 1827–1839.

Betts, A. K., and J. H. Ball, 1998: FIFE surface climate and site-average dataset 1987–89. *J. Atmos. Sci.,* **55,** 1091–1108.

Bottomley, M., C. K. Folland, J. Hsiung, R. E. Newell, and D. E. Parker, 1990: *Global Ocean Surface Temperature Atlas ''GOSTA.''* United Kingdom Meteorological Office/M.I.T., 20 pp.

Bremen, H., and J. J. Kessler, 1995: *Woody Plants in Agro-Ecosystems of Semi-Arid Regions.* Springer-Verlag, 340 pp.

Brunner, J., N. Henninger, U. Deichmann, and B. Ninnin, 1995: West Africa Long Term Perspective Study (WALTPS)—database and user's guide. World Resources Institute, Washington, DC.

Charney, J. G., 1975: Dynamics of deserts and drought in the Sahel. *Quart. J. Roy. Meteor. Soc.,* **101,** 193–202.

——, W. J. Quirk, S. H. Chow, and J. Kornfield, 1977: A comparative study of the effects of albedo change on drought in semi-arid regions. *J. Atmos. Sci.,* **34,** 1366–1385.

Clark, D. B., 1999: Modeling the impact of land surface degradation on the climate of tropical north Africa. Ph.D. thesis, University of Reading, 264 pp. [Available from University of Reading, Whiteknights Road, Reading RG6 6AH, United Kingdom.]

——, Y. K. Xue, R. J. Harding, and P. J. Valdes, 2001: Modeling the impact of land surface degradation on the climate of tropical North Africa. *J. Climate,* **14,** 1809–1822.

Claussen, M., C. Kubatzki, V. Brovkin, A. Ganopolski, P. Hoelzmann, and H. J. Pachur, 1999: Simulation of an abrupt change in Saharan vegetation in the mid-Holocene. *Geophys. Res. Lett.,* **26,** 2037–2040.

Cox, P. M., R. A. Betts, C. B. Bunton, R. L. H. Essery, P. R. Rowntree, and J. Smith, 1999: The impact of new land surface physics on the GCM simulation of climate and climate sensitivity. *Climate Dyn.,* **15,** 183–203.

d'Herbès, J. M., and C. Valentin, 1997: Land surface conditions of the Niamey region: Ecological and hydrological implications. *J. Hydrol.,* **189,** 18–42.

Eltahir, E. A. B., 1998: A soil moisture–rainfall feedback mechanism. 1. Theory and observations. *Water Resour. Res.,* **34,** 765–776.

Fairhead, J., and M. Leach, 1996: *Misreading the African Landscape: Society and Ecology in a Forest-Savanna Mosaic.* Cambridge University Press, 374 pp.

FAO, cited 1995: FAOSTAT—Computerised information series statistics. Food and Agriculture Organization of the United Nations. [Available online at hppt://apps.fao.org.]

Folland, C. K., T. N. Palmer, and D. E. Parker, 1986: Sahel rainfall and worldwide sea temperatures, 1901–85. *Nature,* **320,** 602–607.

Fontaine, B., and S. Janicot, 1996: Sea surface temperature fields associated with West African rainfall anomaly types. *J. Climate,* **9,** 2935–2940.

Garratt, J. R., 1993: Sensitivity of climate simulations to land-surface and atmospheric boundary-layer treatments—A review. *J. Climate,* **6,** 419–449.

Gash, J. H. C., and Coauthors, 1997: The variability of evaporation during the HAPEX-Sahel intensive observation period. *J. Hydrol.,* **189,** 385–399.

Gaze, S. R., J. Brouwer, L. P. Simmonds, and J. Bromley, 1998: Dry season water use patterns under Guiera senegalensis L. shrubs in a tropical savanna. *J. Arid Environ.,* **40,** 53–67.

Gornitz, V., 1985: A survey of anthropogenic vegetation changes in West Africa during the last century—Climatic implications. *Climatic Change,* **7,** 285–325.

Goutorbe, J. P., and Coauthors, 1994: HAPEX-Sahel—A large-scale study of land–atmosphere interactions in the semi-arid tropics. *Ann. Geophys.,* **12,** 53–64.

Goward, S. N., and S. D. Prince, 1995: Transient effects of climate on vegetation dynamics: Satellite observations. *J. Biogeogr.,* **22,** 549–564.

Hanan, N. P., and S. D. Prince, 1997: Stomatal conductance of West-Central Supersite vegetation in HAPEX-Sahel: Measurements and empirical models. *J. Hydrol.,* **189,** 536–562.

Hoffmann, W. A., and R. B. Jackson, 2000: Vegetation–climate feedbacks in the conversion of tropical savanna to grassland. *J. Climate,* **13,** 1593–1602.

Hulme, M., 1992: A 1951–80 global land precipitation climatology for the evaluation of general-circulation models. *Climate Dyn.,* **7,** 57–72.

Lamb, P. J., 1978: Large-scale tropical Atlantic surface circulation patterns associated with subsaharan weather anomalies. *Tellus,* **30A,** 240–251.

Lambin, E. F., and D. Ehrlich, 1997: Land-cover changes in sub-Saharan Africa (1982–1991): Application of a change index based on remotely sensed surface temperature and vegetation indices at a continental scale. *Remote Sens. Environ.,* **61,** 181–200.

——, and Coauthors, 2001: The causes of land-use and -cover change: Moving beyond the myths. *Global Environ. Change,* **11,** 261–269.

Le Houérou, H. N., 1989: *The Grazing Land Ecosystems of the African Sahel.* Springer-Verlag, 282 pp.

Lenhard, R. J., J. C. Parker, and S. Mishra, 1989: On the correspondence between Brooks-Corey and van Genuchten models. *J. Irrig. Drain. Eng.,* **115,** 744–751.

Lindqvist, S., and A. Tengberg, 1993: New evidence of desertification from case-studies in northern Burkina-Faso. *Geogr. Ann.,* **75A,** 127–135.

Loveland, T. R., Z. L. Zhu, D. O. Ohlen, J. F. Brown, B. C. Reed, and L. M. Yang, 1999: An analysis of the IGBP global land-cover characterization process. *Photogramm. Eng. Remote Sens.,* **65,** 1021–1032.

Mabbutt, J. A., and C. Floret, 1980: *Case Studies on Desertification.* UNESCO, 279 pp.

Monteny, B. A., and Coauthors, 1997: The role of the Sahelian biosphere on the water and the CO_2 cycle during the HAPEX-Sahel experiment. *J. Hydrol.,* **189,** 516–535.

Nicholson, S. E., 1989: Long-term changes in African rainfall. *Weather,* **44,** 47–56.

——, C. J. Tucker, and M. B. Ba, 1998: Desertification, drought, and surface vegetation: An example from the West African Sahel. *Bull. Amer. Meteor. Soc.,* **79,** 815–829.

Olsson, K., 1985: Remote sensing for fuelwood resources and land degradation studies in Kordofan, the Sudan. Ph.D. thesis, Royal University of Lund, Lund, Sweden, 182 pp.

Polcher, J., 1995: Sensitivity of tropical convection to land-surface processes. *J. Atmos. Sci.,* **52,** 3143–3161.

Pope, V. D., M. L. Gallani, P. R. Rowntree, and R. A. Stratton, 2000: The impact of new physical parametrizations in the Hadley Centre climate model HadAM3. *Climate Dyn.,* **16,** 123–146.

Prince, S. D., E. B. De Colstoun, and L. L. Kravitz, 1998: Evidence from rain-use efficiencies does not indicate extensive Sahelian desertification. *Global Change Biol.,* **4,** 359–374.

Rowell, D. P., C. K. Folland, K. Maskell, and M. N. Ward, 1995: Variability of summer rainfall over tropical North-Africa (1906–92)—Observations and modeling. *Quart. J. Roy. Meteor. Soc.,* **121,** 669–704.

Scholes, R. J., D. Skole, and J. S. Ingram, 1995: A global database of soil properties: Proposal for implementation. IGBP-DIS Paper 10, 35 pp.

Stephenne, N., and E. F. Lambin, 2001a: A dynamic simulation model of land-use changes in Sudano-sahelian countries of Africa (SALU). *Agric. Ecosyst. Environ.,* **85,** 145–161.

——, and ——, 2001b: Backward land-cover change projections for the Sudano-sahelian countries of Africa with a dynamic simulation model of land-use change (SALU). *Present and Future of Modeling Global Environment Change—Towards Integrated Modeling,* T. Matsuno and H. Kida, Eds., Terra Scientific, 255–270.

Sud, Y. C., and W. M. Lau, 1996: Variability of summer rainfall over tropical North-Africa (1906–92)—Observations and modeling—Comment. *Quart. J. Roy. Meteor. Soc.,* **122,** 1001–1006.

Taylor, C. M., and E. M. Blyth, 2000: Rainfall controls on evaporation at the regional scale: An example from the Sahel. *J. Geophys. Res.,* **105D,** 15 469–15 479.

——, and D. B. Clark, 2001: The diurnal cycle and African easterly waves: A land surface perspective. *Quart. J. Roy. Meteor. Soc.,* **127,** 845–867.

Wang, G. L., and E. A. B. Eltahir, 2000a: Biosphere–atmosphere interactions over West Africa. II: Multiple climate equilibria. *Quart. J. Roy. Meteor. Soc.,* **126,** 1261–1280.

——, and ——, 2000b: Ecosystem dynamics and the Sahel drought. *Geophys. Res. Lett.,* **27,** 795–798.

Xue, Y., 1997: Biosphere feedback on regional climate in tropical north Africa. *Quart. J. Roy. Meteor. Soc.,* **123,** 1483–1515.

——, and J. Shukla, 1993: The influence of land-surface properties on Sahel climate. 1. Desertification. *J. Climate,* **6,** 2232–2245.

——, P. J. Sellers, J. L. Kinter, and J. Shukla, 1991: A simplified biosphere model for global climate studies. *J. Climate,* **4,** 345–364.

Zeng, N., J. D. Neelin, K. M. Lau, and C. J. Tucker, 1999: Enhancement of interdecadal climate variability in the Sahel by vegetation interaction. *Science,* **286,** 1537–1540.

Zheng, X. Y., and E. A. B. Eltahir, 1997: The response to deforestation and desertification in a model of West African monsoons. *Geophys. Res. Lett.,* **24,** 155–158.